Can Probability Maps of Swept-Source Optical Coherence Tomography Predict Visual Field Changes in Preperimetric Glaucoma?

Won June Lee,[1,2] Young Kook Kim,[1,2] Jin Wook Jeoung,[1,2] and Ki Ho Park[1,2]

[1]Department of Ophthalmology, Seoul National University College of Medicine, Seoul, Korea
[2]Department of Ophthalmology, Seoul National University Hospital, Seoul, Korea

Correspondence: Ki Ho Park, Department of Ophthalmology, Seoul National University Hospital, Seoul National University College of Medicine, 101 Daehak-ro, Jongno-gu, Seoul 03080, Korea; kihopark@snu.ac.kr.

Submitted: July 26, 2017
Accepted: November 9, 2017

Citation: Lee WJ, Kim YK, Jeoung JW, Park KH. Can probability maps of swept-source optical coherence tomography predict visual field changes in preperimetric glaucoma? *Invest Ophthalmol Vis Sci*. 2017;58:6257–6264. DOI:10.1167/iovs.17-22697

Purpose. To determine the usefulness of swept-source optical coherence tomography (SS-OCT) probability maps in detecting locations with significant reduction in visual field (VF) sensitivity or predicting future VF changes, in patients with classically defined preperimetric glaucoma (PPG).

Methods. Of 43 PPG patients, 43 eyes were followed-up on every 6 months for at least 2 years were analyzed in this longitudinal study. The patients underwent wide-field SS-OCT scanning and standard automated perimetry (SAP) at the time of enrollment. With this wide-scan protocol, probability maps originating from the corresponding thickness map and overlapped with SAP VF test points could be generated. We evaluated the vulnerable VF points with SS-OCT probability maps as well as the prevalence of locations with significant VF reduction or subsequent VF changes observed in the corresponding damaged areas of the probability maps.

Results. The vulnerable VF points were shown in superior and inferior arcuate patterns near the central fixation. In 19 of 43 PPG eyes (44.2%), significant reduction in baseline VF was detected within the areas of structural change on the SS-OCT probability maps. In 16 of 43 PPG eyes (37.2%), subsequent VF changes within the areas of SS-OCT probability map change were observed over the course of the follow-up.

Conclusions. Structural changes on SS-OCT probability maps could detect or predict VF changes using SAP, in a considerable number of PPG eyes. Careful comparison of probability maps with SAP results could be useful in diagnosing and monitoring PPG patients in the clinical setting.

Keywords: OCT probability map, structure–function relationship, preperimetric glaucoma, swept-source optical coherence tomography, wide-field

Glaucoma is an optic neuropathy characterized by retinal ganglion cell (RGC) degeneration that leads to visual field (VF) loss.[1] Thinning of retinal nerve fiber layer (RNFL) thickness is an early sign of glaucoma, and a significant reduction in the number of RGCs can occur before VF defect is detected.[2–7] As imaging modalities have evolved, clinicians have frequently faced early-glaucoma diagnostic challenges with patients whose structural examinations are characterized by suspicious glaucomatous-change findings (e.g., RNFL thinning or enlarged cupping) but for whom the results of functional examination are uncertain. Recently, the term "preperimetric glaucoma (PPG)" has been coined to define glaucomatous eyes that, notwithstanding the characteristic structural changes, lack VF loss based on conventional standard automated perimetry (SAP).

The structure–function relationship in glaucoma has been a focus in many studies.[8–13] The report by Hood et al.[14–19] summarizing the data from optical coherence tomography (OCT) macular and disc cube scans allows for direct comparison with the results of VF tests.[14–19] This commercially available method (which is available in all countries where equipment and software are purchased) provides probability maps based on swept-source OCT (SS-OCT) RNFL and macular–structural imaging analysis, on which maps the structural changes are superimposed with the SAP VF locations. With these maps, the damaged area detected by SS-OCT can be compared directly with possible VF damage, topographically. And as SS-OCT has evolved, provision of wide-field RNFL maps for use with probability maps has become possible.

Preperimetric glaucoma patients have, according to the definition of their condition, structural changes but also functional changes not meeting the conventional criteria of abnormality. However, according to the probability maps provided by Hood et al.,[14–19] there might be functional changes that correspond to structural changes but that might nonetheless go undetected, due to the small area of examination or to functional-test sensitivity and/or specificity limitations. Thus, we hypothesized that VF areas corresponding to probability map–indicated structural changes have either significant reduction in baseline VF sensitivity or subsequent VF changes arising during the follow-up period.

The purpose of this study was to evaluate the VF test points vulnerable to structural change using SS-OCT probability maps and to determine these maps' usefulness for detection of significant reduction in baseline VF sensitivity or prediction of future VF changes, in patients with PPG.

Methods

Participants

For this longitudinal study, we enrolled patients with PPG (43 eyes). All of the participants had visited the Glaucoma Clinic of Seoul National University Hospital from August 2014 through May 2015 and been enrolled in the Macular Ganglion Cell Imaging Study, an ongoing prospective study designed in 2011. The study protocol, approved by the institutional review board of Seoul National University Hospital, adhered to the tenets of the Declaration of Helsinki.

Each patient underwent a comprehensive ophthalmic examination, including a medical history review, slit-lamp biomicroscopy, IOP measurement using Goldmann applanation tonometry, gonioscopy, disc examination using a 90-diopter (D) lens, color fundus, and disc photography as well as red-free fundus photography (VX-10; Kowa Optimed, Tokyo, Japan), SAP 24-2 testing (Humphrey Field Analyzer; Carl Zeiss Meditec, Dublin, CA, USA), and SS-OCT (DRI-OCT-1 Atlantis, Topcon, Tokyo, Japan).

The PPG diagnosis was made based on the presence of one or more localized RNFL defects corresponding to characteristic glaucoma optic disc changes defined on stereo disc photography as an inter-eye cup-to-disc (C/D) ratio difference >0.2, increased cupping (>0.7 vertical C/D ratio), neuroretinal rim thinning, notching, or excavation.[20–22] All of the disc and RNFL photography images were evaluated by two glaucoma specialists (YKK, JWJ) in a masked fashion. Discrepancies between the observers were resolved by consensus or adjudication by a third glaucoma specialist (KHP). Patients were required to have an SAP result not meeting the conventional criteria of glaucomatous VF at the initial examination. Eyes with glaucomatous VF defects were defined as those with a cluster of three points with probabilities of <5% on the pattern deviation map in at least one hemifield, including at least one point with a probability of <1%, or those with a cluster of two points with a probability of <1%, and a glaucoma hemifield test (GHT) result outside 99% of age-specific normal limits or a pattern standard deviation (PSD) outside 95% of normal limits. All VF defects were confirmed on two consecutive reliable tests.[23]

The inclusion criteria were as follows: (1) PPG in one or both eyes at the first clinic visit, (2) no history of IOP-lowering treatment use, (3) follow-up examination attendance every 6 months for at least 2 years, and (4) no treatment or treatment with only topical medications during the follow-up period. Additionally, patients to be included in the study had to have a best-corrected visual acuity of 20/40 or better, spherical equivalent refractive errors between +6.0 and −6.0 D, cylinder correction <3.0 D, and an open anterior chamber angle. All of the SS-OCT images referenced had an image quality score of 50 or better. For cases in which both eyes met all of the eligibility criteria, one eye was randomly chosen as the study eye.

Wide-Field Swept-Source Optical Coherence Tomography: Hood Report

All of the patients underwent SS-OCT imaging performed by one experienced technician. Retinal nerve fiber layer (RNFL) measurement and macular ganglion cell analysis were performed according to the right-eye orientation.

With regard to SS-OCT, the wide-field scan protocol was applied to obtain the wide-field RNFL thickness map. Thereby, it was possible to obtain images of the macular and optic nerve head regions in a single scan, for a total acquisition time of only 1.3 seconds. The 12 × 9 mm scan comprised 256 B-scans, each in turn comprising 512 A-scans, for a total of 131,072 axial scans/volume.

With the built-in analysis software (version 9.30; Topcon, Tokyo, Japan), the RNFL boundary was automatically segmented and the RNFL thickness throughout the scan was calculated. The RNFL thickness map was generated within the 12 × 9-mm field area with color scales corresponding to numeric RNFL thickness measurements. A macular ganglion cell–inner plexiform layer (GC-IPL) thickness map within a 6.0 × 6.0-mm^2 macular area also was generated. With this wide-scan protocol, a "3-dimensional wide glaucoma report with VF test points (Hood report)" could be generated. This report provides the RNFL probability map and macular GC-IPL probability map, which are drawn according to corresponding thickness maps by comparing the patients' thickness values with those of an age-similar healthy normative database and overlapping them with VF test points SAP 24-2 and SAP 10-2, respectively. The wide-field scan protocol set the center of image acquisition between the disc and macula as the default, and the probability map could be generated based on the normative database obtained by the same method. The probability maps indicate the significance level on a continuous color scale from green ($P > 0.1$) to dark red ($P < 0.001$), yellow, red, and dark red indicating probabilities of 0.05, 0.01, and <0.001, respectively.[14–16] In this study, we determined structural changes on probability map according to the yellow and red VF test point significances ($P < 0.05$).

Definitions of Visual Field Changes on Standard Automated Perimetry

Unlike the case of glaucomatous VF defect, which was defined at the time of glaucoma diagnosis, we arbitrarily defined VF change at baseline and during follow-up. VF change at baseline was defined as the presence of VF test points on the pattern deviation map with probabilities <5%; VF change during follow-up was defined as the presence of VF points deteriorating more than the lower 5th percentile of test–retest variability of baseline sensitivities depicted on the Guided Progression Analysis (GPA) follow-up maps. The VF changes were evaluated at each VF test point. VF progression was determined according to the Early Manifest Glaucoma Trial (EMGT) criteria. The GPA software provides a plain-language report of "possible progression" if two consecutive fields show that the same three or more points changed from the baseline, or "likely progression" if three consecutive fields show change at the same three or more points, based on the EMGT progression criteria.[24] In this study, "likely progression" or "possible progression" were considered to indicate VF progression.

Definitions of Topographic Agreement

We arbitrarily defined topographic agreement between SS-OCT probability maps and VF tests as more than two VF points being within the areas of structural change on the SS-OCT probability maps. In addition, the following ratios were calculated for determination of topographic matching between SS-OCT probability maps and VF tests.

$$\frac{\text{Number of damaged VF points overlapped in both SS OCT and VF test}}{\text{Number of VF points damaged in SS OCT probability map or VF test}}$$

$$\frac{\text{Number of damaged VF points overlapped in both SS OCT and VF test}}{\text{Number of VF points damaged in SS OCT probability map}}$$

Statistical Analysis

From the enrolled PPG eyes' probability maps, we calculated the frequency of each VF test point showing structural

Table 1. Demographic Characteristics of Enrolled Preperimetric Glaucoma Eyes

	Preperimetric Glaucoma, $N = 43$
Age (y)	58.23 ± 10.64 (32–78)
IOP (mm Hg)	12.55 ± 2.23 (9–19)
Spherical equivalent (D)	−1.59 ± 2.81 (−5.25 to 1.50)
Baseline visual field	
Mean deviation (dB)	0.14 ± 1.29 (−2.05 to 2.27)
Pattern standard deviation (dB)	1.80 ± 0.47 (1.00–3.19)
Visual field index (%)	99.32 ± 0.68 (98–100)
Follow-up duration (mo)	29.12 ± 4.54 (24–35)

The data are shown as the mean ± standard deviation (range).

changes. Also, we obtained the distribution for the vulnerable zone that showed a high frequency of structural change on the probability map. From the baseline SAP 24-2 and GPA during the follow-up period, we calculated the frequency of each VF test point showing VF changes.

Among the enrolled eyes, the prevalence of significant reduction in baseline VF sensitivity as well as the prevalence of VF changes shown (in the GPA analysis) within the structural changes on the probability maps were calculated. The prevalence of topographic agreement, as defined above, also was calculated. For comparison between the structural changes on the probability maps and the VF changes, the RNFL probability map was used.

All of the statistical tests were performed using PASW Statistics 18 (SPSS, Chicago, IL, USA).

Results

Of 43 patients with PPG 43 eyes were included in the analyses. Initially, 120 glaucoma patients were selected, and 74 patients showing glaucomatous VF damage (perimetric glaucoma) were excluded. Then, three PPG patients who were not followed-up on for more than 24 months were excluded. Table 1 summarizes the demographic characteristics of the enrolled patients. The mean age was 58.23 ± 10.64 years. The baseline mean MD and PSD were 0.14 ± 1.29 and 1.80 ± 0.47 dB, respectively.

Distribution of Structural Changes on Probability Map of Swept-Source Optical Coherence Tomography in Preperimetric Glaucoma Eyes

The frequency of structural change on the RNFL probability map is plotted in Figure 1A. The VF points with a frequency of over 20% (red) are shown in superior and inferior arcuate patterns near the central fixation. The frequency of structural change on the GC-IPL probability map, meanwhile, is plotted in Figure 1B. The VF points with a frequency of over 20% (red) are shown near the central fixation.

Visual Field Change Detection on Probability Map of Swept-Source Optical Coherence Tomography

Figures 2 and 3 (Cases 1 and 2) and Supplementary Figures S1 and S2 (Cases 3 and 4) show representative cases in which PPG patients' VF changes were detected in the areas of structural change on SS-OCT probability maps. In 19 of 43 PPG eyes (44.2%), significant reduction in baseline VF was detected in the areas of structural change on the SS-OCT probability maps (Cases 1–4). In 16 of 43 PPG eyes (37.2%), VF changes noted in the GPA analysis during follow-up occurred in the areas of structural change on the SS-OCT probability maps (Cases 2–4). During the follow-up, seven eyes (16.3%) showed VF progression in the GPA analysis.

Topographic Agreement

Topographic agreement between SS-OCT probability maps and VF test is summarized in Table 2. In five of 43 PPG eyes (11.6%), topographic agreement between locations with

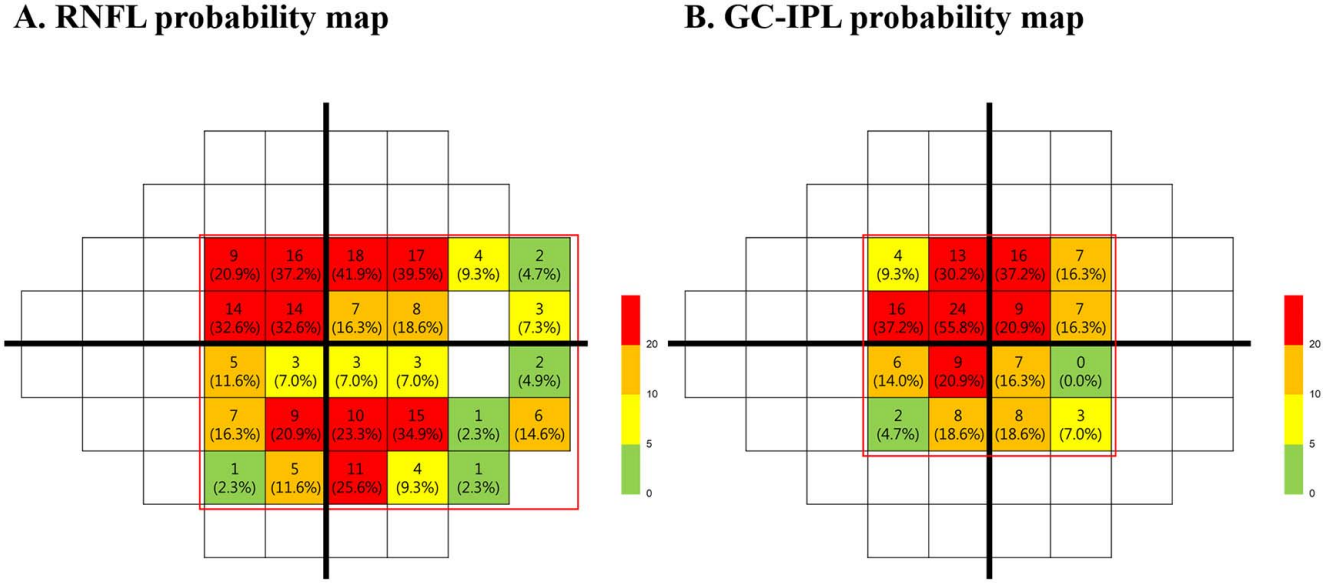

Figure 1. Distribution of structural changes on probability map of SS-OCT in PPG eyes. The vulnerable VF points of PPG eyes were shown on SS-OCT probability maps. (**A**) The RNFL probability map showed the vulnerable VF points in the superior and inferior arcuate patterns near the fixation. (**B**) The GC-IPL probability map showed the vulnerable VF points with a frequency of over 20% (*red*) near the central fixation. The number displayed at each VF point represents the number of eyes showing structural change on the probability maps. The frequency is indicated in parentheses.

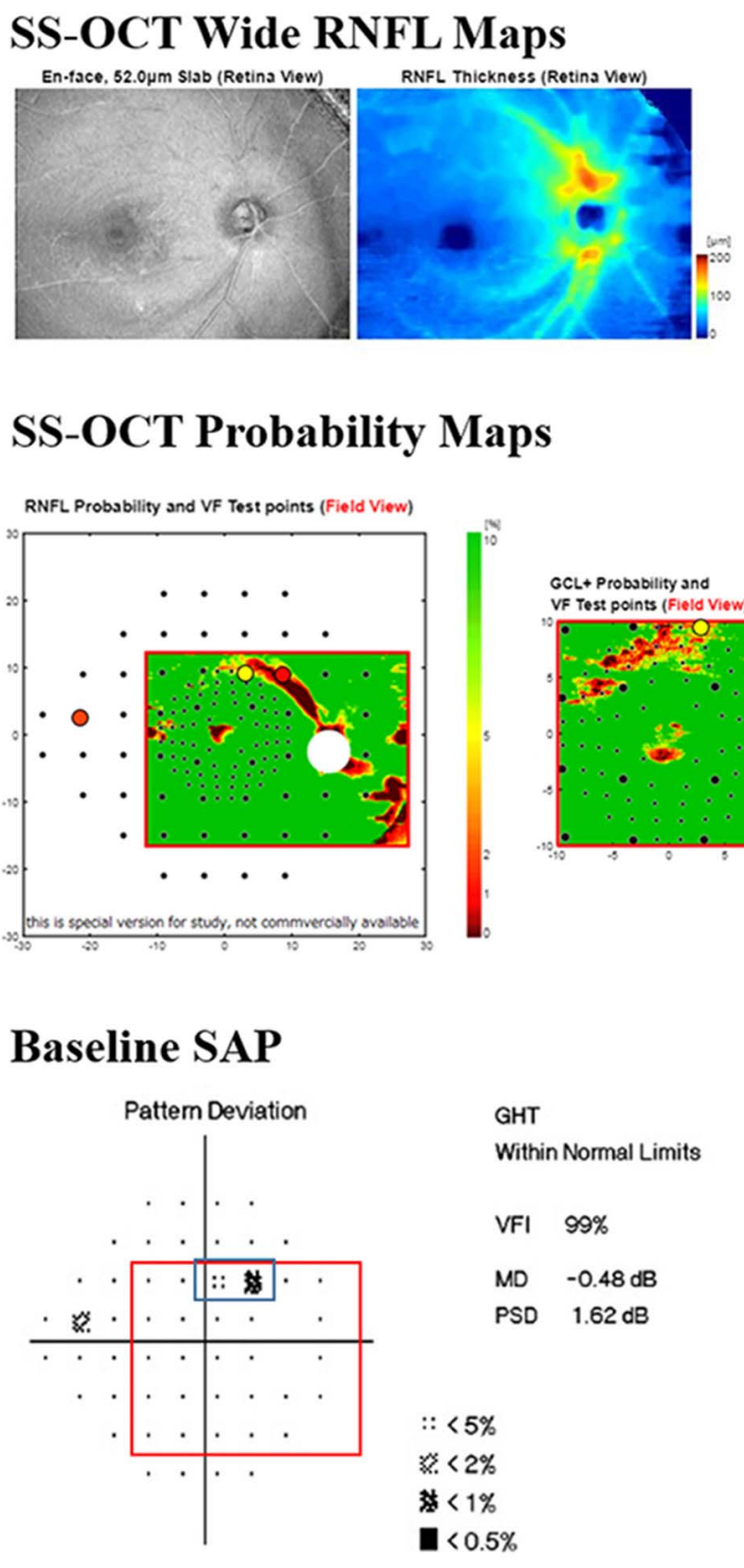

Figure 2. Case 1 of a 69-year-old man with PPG in right eye. The wide-field SS-OCT RNFL thickness map clearly showed inferotemporal RNFL defects. VF changes in baseline SAP were shown within the areas of the SS-OCT RNFL probability map's structural change (*blue squares*). VF points showing decreased sensitivity at baseline SAP were marked on the SS-OCT probability maps as colored circles. Only 24-2 SAP was performed in this study. The 10-2 VF points shown in the figure were generated automatically with the SS-OCT built-in software.

Investigative Ophthalmology & Visual Science

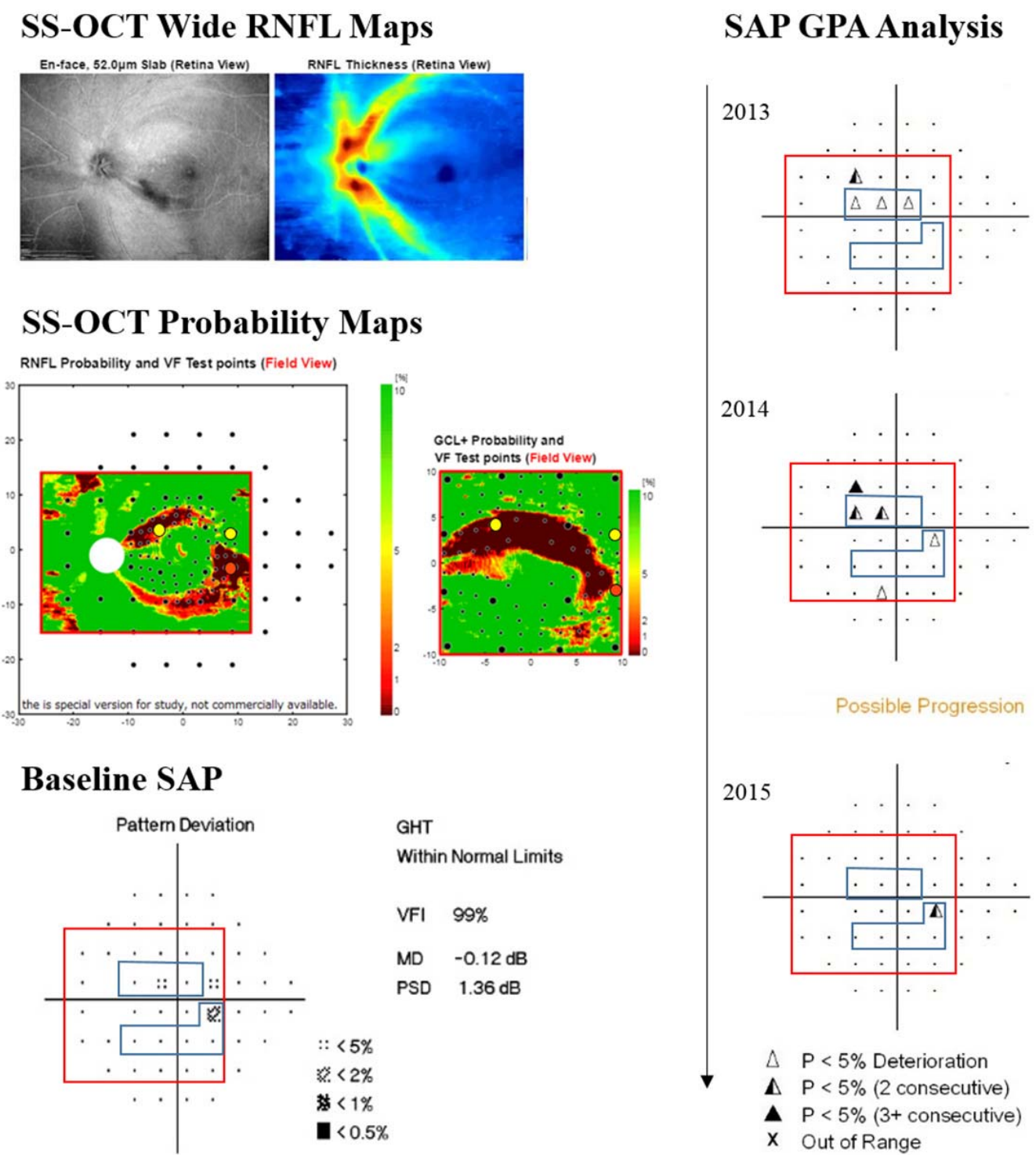

FIGURE 3. Case 2 of a 59-year-old man with PPG in left eye. The wide-field SS-OCT RNFL thickness map clearly showed superotemporal and inferotemporal RNFL defects. VF changes in baseline SAP were shown within the areas of the SS-OCT probability maps' structural change (*blue squares*). In the GPA, some of the VF changes were included in the areas of the SS-OCT RNFL probability map's structural change (*blue squares*). VF points showing decreased sensitivity at baseline SAP were marked on the SS-OCT probability maps as *colored circles*. Only 24-2 SAP was performed in this study. The 10-2 VF points shown in the figure were generated automatically with the SS-OCT built-in software.

significant reduction in sensitivity at the baseline VF test and areas of structural change on the SS-OCT probability maps was shown. In eight of 43 PPG eyes (18.6%), topographic agreement between VF changes noted in the GPA analysis during follow-up and areas of structural change on the SS-OCT probability maps was shown.

Distribution of Visual Field Changes on Standard Automated Perimetry

The frequency of VF changes on SAP is plotted in Figure 4. Figure 4A shows the frequency of VF changes at the baseline SAP, and Figure 4B indicates the frequency of VF

Table 2. Topographic Agreement Between Structural Changes on SS-OCT Probability Map and Locations With Significant Reduction in Baseline VF Sensitivity or VF Changes on GPA Maps

	Mean ± SD (Range)
Significant reduction in baseline SAP VF test*	
Numbers of changed VF points within area of SS-OCT probability map damage	0.47 ± 0.77 (0–3)
Overlapped VF points / VF points damaged in VF test or SS-OCT	0.07 ± 0.12 (0–0.43)
Overlapped VF points / VF points damaged on SS-OCT probability map	0.09 ± 0.17 (0–0.67)
Topographic agreement†	5/43 (11.6%)‡
GPA VF changes§	
Numbers of changed VF points within the area of SS-OCT probability map damage	0.58 ± 0.98 (0–4)
Overlapped VF points / VF points damaged in VF test or SS-OCT	0.07 ± 0.11 (0–0.50)
Overlapped VF points / VF points damaged on SS-OCT probability map	0.12 ± 0.18 (0–0.57)
Topographic agreement†	8/43 (18.6%)‡

* Presence of VF test points on pattern deviation map with probabilities <5%.

† More than 2 VF points within area of SS-OCT damage.

‡ The data are shown as patient number/total (%).

§ Presence of VF points deteriorating more than lower 5th percentile of test-retest variability of baseline sensitivities depicted on GPA follow-up maps.

changes detected in the GPA analysis during the follow-up period.

Discussion

In the present study, we evaluated VF test points vulnerable to structural change with SS-OCT probability maps, and we determined the usefulness of those maps in detecting VF changes in PPG patients—a group of patients for whom management is highly subjective and challenging. To our knowledge, this is the first study to apply commercially available SS-OCT probability maps to PPG patients.

Some reports show that VF defect progresses during follow-up in approximately 50% to 60% PPG patients,[20,21,25] though results vary with follow-up duration. For the purposes of diagnosis and prediction of VF progression in such PPG patients, recent studies have evaluated the usefulness of advanced OCT technology. Zhang et al.[26] reported that the Fourier-domain OCT parameters at the baseline visit, especially those affecting the macula (focal loss volume of RNFL+GC-IPL parameter), can predict the development of glaucomatous VF loss in PPG patients. Recently, our group reported on the usefulness of the SS-OCT wide-field RNFL thickness map in distinguishing eyes with PPG from healthy eyes.[27]

With the advent of newer technology, there have been efforts to topographically compare abnormal regions as seen on OCT with those observed in VFs. The structure–function relationship has been a focus in many studies; Hood et al.,[14–19] for example, recently developed a probability map (the Hood report) that makes possible the comparison of local RGC and RNFL loss with local loss in VF sensitivities. In this respect, newly developed SS-OCT and its wide-field scan protocol can show a 12 × 9 mm-wide area, including the optic disc and macula, on a single-page printout. With this wide-field scan, probability maps can be generated. Using SS-OCT probability maps, we endeavored to examine the structure–function relationship in PPG patients.

Our study revealed that the SS-OCT probability map could detect significant reduction in baseline VF sensitivity as well as predict the future progression of those changes. Although topographic concordance between the probability map and the corresponding SAP result was not statistically confirmed and frequency maps were not clearly matched, baseline VF changes or decreased sensitivity relative to the baseline VF were detected in the area of the SS-OCT probability maps' structural changes in a significant number of PPG patients. This result can be interpreted in two ways.

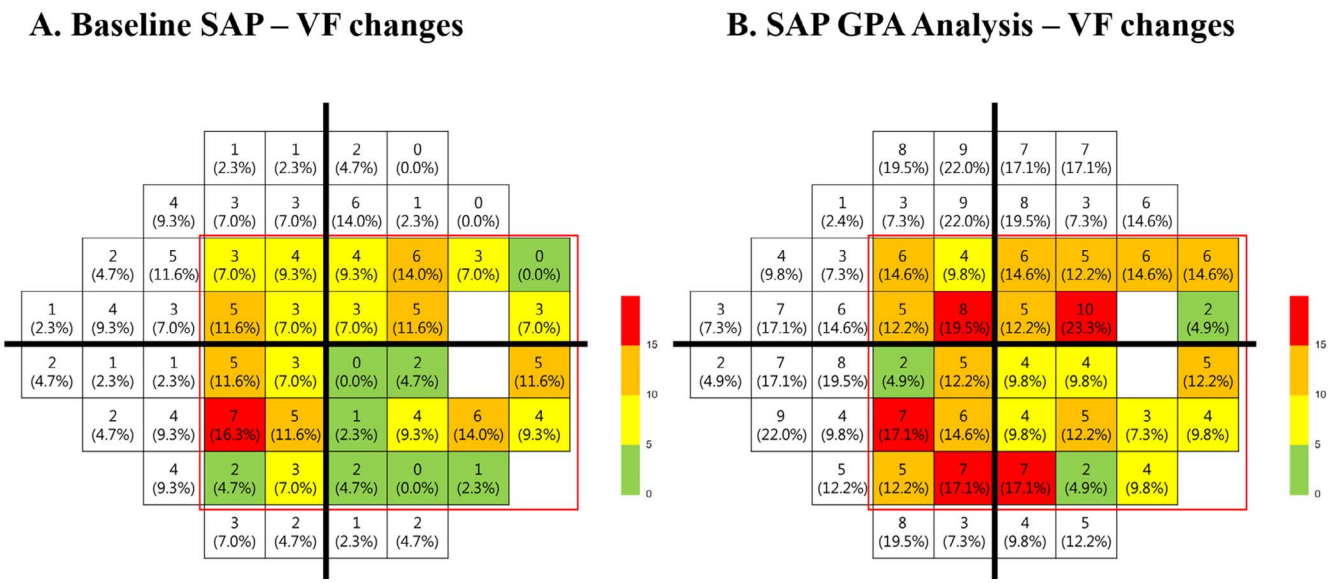

Figure 4. Distribution of VF changes on SAP. The frequencies of VF changes on SAP were shown: (**A**) frequency of VF changes at baseline SAP; (**B**) frequency of VF changes detected by GPA during follow-up period.

First, PPG usually has been diagnosed according to the classical definition of VF change, fine VF changes not meeting the classical definition for perimetric glaucoma generally being ignored; however, such VF changes are meaningful if they topographically match the probability maps. Recently, one group, considering the diagnosis of "glaucoma" in cases where OCT probability plots show an abnormality in a region corresponding to a defect seen in the VF, reported that with this criterion, glaucomatous damages are often missed during clinical evaluation.[28] Analysis of integral structural and functional relationships in early glaucoma will continue to be needed into the future. Preperimetric glaucoma (PPG) might prove to be an artificial definition of very early glaucoma, and if so, a change in the concept of PPG will be necessary.

Second, SS-OCT probability maps can be predictive of subsequent VF change. In most patients, anatomic damage can be detected earlier than functional damage.[29,30] Swept- source OCT probability maps can detect very early glaucomatous damage at the cusp of being detectable on an SAP test.[26] Significantly therefore, they can identify glaucoma patients who have progressed from PPG to perimetric glaucoma.

Recently, the macular inner retinal structures, including parameters related to the GC-IPL, have been successfully used to evaluate glaucoma status in the clinical setting. In addition, many studies have shown the glaucoma-diagnostic performance of GC-IPL parameters to be comparable to or better than that of RNFL parameters.[16,31–34] In the present results, the overlapped four red VF points common to the RNFL and GC-IPL probability maps (Figs. 1A, 1B) were distributed in superior arcuate patterns near the fixation. Those vulnerable VF points in PPG eyes coincided with the macular vulnerable zone (MVZ) of Hood[17] as well as with the inferior macular GC-IPL reduction area in studies of Kim et al.[35,36] that evaluated the temporal relationship between macular GC-IPL and circumpapillary RNFL loss.

Several points need to be considered when interpreting the results of the current study. First, the definition of VF change and topographic agreement between SS-OCT probability maps and VF test were arbitrary. In light of the long-term fluctuation of VF results, identification of significant reduction in baseline VF sensitivity based only on a one-time baseline VF test can be questioned.[37–40] Also, in GPA analysis, it might be considered controversial to define VF change as the point at which significant sensitivity changes are observed relative to the baseline for each test, as the false-positive value might be high. For these reasons, the topographic relationship at each VF test point between the probability map and the SAP results might not be statistically significant. Future studies with large numbers of SAP results will be needed in order to define more reliable VF changes. Second, because the VF test points in the present study were distributed sparsely, the early RNFL defects passing between the VF points might not have been detected by the VF tests. Third, in this study, we compared the RNFL probability map only with SAP 24-2, because we did not obtain the SAP 10-2. But it is well known that the macular GC-IPL probability map is related to the central VF; therefore, its comparison with SAP 10-2 would be more suitable for evaluation of fine central VF changes.[41] Further study comparing the GC-IPL probability map with SAP 10-2 would be needed. Fourth, because the software does not provide the objective probability values of each pixel, determination of structural change according to only color change at the VF point could be ambiguous. Further, results could vary with VF point size. Fifth, although the SS-OCT provided a wide 12 × 9-mm scan, no assessment was made of VF points outside the probability maps. With this map, evaluation of the nasal step part, where field change occurs frequently, is impossible.

Despite these limitations, the structural changes on the SS-OCT probability maps could detect or predict, in considerably PPG eyes, the VF changes using SAP. Careful comparison of SS-OCT probability maps with SAP VF test results could be key to the evaluation of early-stage glaucomatous eyes, such as those with PPG.

Acknowledgments

Disclosure: **W.J. Lee**, None; **Y.K. Kim**, None; **J.W. Jeoung**, None; **K.H. Park**, None

References

1. Weinreb RN, Aung T, Medeiros FA. The pathophysiology and treatment of glaucoma: a review. *JAMA*. 2014;311:1901–1911.
2. Hirooka K, Manabe S, Tenkumo K, Nitta E, Sato S, Tsujikawa A. Use of the structure-function relationship in detecting glaucoma progression in early glaucoma. *BMC Ophthalmol*. 2014;14:118.
3. Hood DC, Kardon RH. A framework for comparing structural and functional measures of glaucomatous damage. *Prog Retin Eye Res*. 2007;26:688–710.
4. Quigley HA, Katz J, Derick RJ, Gilbert D, Sommer A. An evaluation of optic disc and nerve fiber layer examinations in monitoring progression of early glaucoma damage. *Ophthalmology*. 1992;99:19–28.
5. Tuulonen A, Airaksinen PJ, Montagna A, Nieminen H. Screening for glaucoma with a non-mydriatic fundus camera. *Acta Ophthalmol*. 1990;68:445–449.
6. Sommer A. Retinal nerve fiber layer. *Am J Ophthalmol*. 1995; 120:665–667.
7. Sommer A, Miller NR, Pollack I, Maumenee AE, George T. The nerve fiber layer in the diagnosis of glaucoma. *Arch Ophthalmol*. 1977;95:2149–2156.
8. Garway-Heath DF, Poinoosawmy D, Fitzke FW, Hitchings RA. Mapping the visual field to the optic disc in normal tension glaucoma eyes. *Ophthalmology*. 2000;107:1809–1815.
9. Malik R, Swanson WH, Garway-Heath DF. 'Structure-function relationship' in glaucoma: past thinking and current concepts. *Clin Exp Ophthalmol*. 2012;40:369–380.
10. Hood DC, Anderson SC, Wall M, Kardon RH. Structure versus function in glaucoma: an application of a linear model. *Invest Ophthalmol Vis Sci*. 2007;48:3662–3668.
11. Hood DC, Anderson SC, Wall M, Raza AS, Kardon RH. A test of a linear model of glaucomatous structure-function loss reveals sources of variability in retinal nerve fiber and visual field measurements. *Invest Ophthalmol Vis Sci*. 2009;50:4254–4266.
12. Leite MT, Zangwill LM, Weinreb RN, Rao HL, Alencar LM, Medeiros FA. Structure-function relationships using the Cirrus spectral domain optical coherence tomograph and standard automated perimetry. *J Glaucoma*. 2012;21:49–54.
13. Raza AS, Hood DC. Evaluation of the structure-function relationship in glaucoma using a novel method for estimating the number of retinal ganglion cells in the human retina. *Invest Ophthalmol Vis Sci*. 2015;56:5548–5556.
14. Hood DC, De Cuir N, Blumberg DM, et al. A single wide-field OCT protocol can provide compelling information for the diagnosis of early glaucoma. *Trans Vis Sci Tech*. 2016;5(6):4.
15. Hood DC, Fortune B, Mavrommatis MA, et al. Details of glaucomatous damage are better seen on OCT en face images than on OCT retinal nerve fiber layer thickness maps. *Invest Ophthalmol Vis Sci*. 2015;56:6208–6216.
16. Hood DC, Raza AS, de Moraes CG, Liebmann JM, Ritch R. Glaucomatous damage of the macula. *Prog Retin Eye Res*. 2013;32:1–21.

17. Hood DC. Improving our understanding, and detection, of glaucomatous damage: an approach based upon optical coherence tomography (OCT). *Prog Retin Eye Res*. 2017;57:46–75.
18. Hood DC, Raza AS. Method for comparing visual field defects to local RNFL and RGC damage seen on frequency domain OCT in patients with glaucoma. *Biomed Opt Express*. 2011;2:1097–1105.
19. Hood DC, Raza AS. On improving the use of OCT imaging for detecting glaucomatous damage. *Br J Ophthalmol*. 2014;98(suppl 2):ii1–ii9.
20. Jeong JH, Park KH, Jeoung JW, Kim DM. Preperimetric normal tension glaucoma study: long-term clinical course and effect of therapeutic lowering of intraocular pressure. *Acta Ophthalmol*. 2014;92:e185–e193.
21. Kim KE, Jeoung JW, Kim DM, Ahn SJ, Park KH, Kim SH. Long-term follow-up in preperimetric open-angle glaucoma: progression rates and associated factors. *Am J Ophthalmol*. 2015;159:160–168.
22. Seol BR, Jeoung JW, Park KH. Glaucoma detection ability of macular ganglion cell-inner plexiform layer thickness in myopic preperimetric glaucoma. *Invest Ophthalmol Vis Sci*. 2015;56:8306–8313.
23. Anderson D, Patella V. *Automated Static Perimetry*. 2nd ed. St. Louis: Mosby; 1999.
24. Leske MC, Heijl A, Hyman L, Bengtsson B. Early Manifest Glaucoma Trial: design and baseline data. *Ophthalmology*. 1999;106:2144–2153.
25. Sawada A, Manabe Y, Yamamoto T, Nagata C. Long-term clinical course of normotensive preperimetric glaucoma [published online ahead of print April 17, 2017]. *Br J Ophthalmol*. doi: 10.1136/bjophthalmol-2016-309401.
26. Zhang X, Loewen N, Tan O, et al. Predicting development of glaucomatous visual field conversion using baseline fourier-domain optical coherence tomography. *Am J Ophthalmol*. 2016;163:29–37.
27. Lee WJ, Na KI, Kim YK, Jeoung JW, Park KH. Diagnostic ability of wide-field retinal nerve fiber layer maps using swept-source optical coherence tomography for detection of preperimetric and early perimetric glaucoma. *J Glaucoma*. 2017;26:577–585.
28. Alhadeff PA, De Moraes CG, Chen M, Raza AS, Ritch R, Hood DC. The association between clinical features seen on fundus photographs and glaucomatous damage detected on visual fields and optical coherence tomography scans. *J Glaucoma*. 2017;26:498–504.
29. Johnson CA, Sample PA, Zangwill LM, et al. Structure and function evaluation (SAFE): II. Comparison of optic disk and visual field characteristics. *Am J Ophthalmol*. 2003;135:148–154.
30. Kuang TM, Zhang C, Zangwill LM, Weinreb RN, Medeiros FA. Estimating lead time gained by optical coherence tomography in detecting glaucoma before development of visual field defects. *Ophthalmology*. 2015;122:2002–2009.
31. Jeong JH, Choi YJ, Park KH, Kim DM, Jeoung JW. Macular ganglion cell imaging study: covariate effects on the spectral domain optical coherence tomography for glaucoma diagnosis. *PLoS One*. 2016;11:e0160448.
32. Jeoung JW, Choi YJ, Park KH, Kim DM. Macular ganglion cell imaging study: glaucoma diagnostic accuracy of spectral-domain optical coherence tomography. *Invest Ophthalmol Vis Sci*. 2013;54:4422–4429.
33. Mwanza JC, Durbin MK, Budenz DL, et al. Glaucoma diagnostic accuracy of ganglion cell-inner plexiform layer thickness: comparison with nerve fiber layer and optic nerve head. *Ophthalmology*. 2012;119:1151–1158.
34. Lee WJ, Kim YK, Park KH, Jeoung JW. Trend-based analysis of ganglion cell-inner plexiform layer thickness changes on optical coherence tomography in glaucoma progression. *Ophthalmology*. 2017;124:1383–1391.
35. Kim YK, Ha A, Na KI, Kim HJ, Jeoung JW, Park KH. Temporal relation between macular ganglion cell-inner plexiform layer loss and peripapillary retinal nerve fiber layer loss in glaucoma. *Ophthalmology*. 2017;124:1056–1064.
36. Kim YK, Jeoung JW, Park KH. Inferior macular damage in glaucoma: its relationship to retinal nerve fiber layer defect in macular vulnerability zone. *J Glaucoma*. 2017;26:126–132.
37. Boeglin RJ, Caprioli J, Zulauf M. Long-term fluctuation of the visual field in glaucoma. *Am J Ophthalmol*. 1992;113:396–400.
38. Fogagnolo P, Sangermani C, Oddone F, et al. Long-term perimetric fluctuation in patients with different stages of glaucoma. *Br J Ophthalmol*. 2011;95:189–193.
39. Hutchings N, Wild JM, Hussey MK, Flanagan JG, Trope GE. The long-term fluctuation of the visual field in stable glaucoma. *Invest Ophthalmol Vis Sci*. 2000;41:3429–3436.
40. Tattersall CL, Vernon SA, Menon GJ. Mean deviation fluctuation in eyes with stable Humphrey 24-2 visual fields. *Eye (Lond)*. 2007;21:362–366.
41. De Moraes CG, Hood DC, Thenappan A, et al. 24-2 visual fields miss central defects shown on 10-2 tests in glaucoma suspects, ocular hypertensives, and early glaucoma. *Ophthalmology*. 2017;124:1449–1454.

Investigative Ophthalmology & Visual Science